ISSN 0081-5438, Proceedings of the Steklov Institute of Mathematics, 2018, Vol. 300, pp. 34–55. © Pleiades Publishing, Ltd., 2018.
Original Russian Text © V.V. Vedeneev, A.B. Poroshina, 2018, published in Trudy Matematicheskogo Instituta imeni V.A. Steklova, 2018, Vol. 300, pp. 42–64.

Stability of an Elastic Tube Conveying a Non-Newtonian Fluid and Having a Locally Weakened Section

V. V. Vedeneev[a] **and A. B. Poroshina**[b]

Received September 15, 2017

Abstract—The work is devoted to the stability analysis of the flow of a non-Newtonian power-law fluid in an elastic tube. Integrating the equations of motion over the cross section, we obtain a one-dimensional equation that describes long-wave low-frequency motions of the system in which the rheology of the flowing fluid is taken into account. In the first part of the paper, we find a stability criterion for an infinite uniform tube and an absolute instability criterion. We show that instability under which the axial symmetry of motion of the tube is preserved is possible only for a power-law index of $n < 0.611$, and absolute instability is possible only for $n < 1/3$; thus, after the loss of stability of a linear viscous medium, the flow cannot preserve the axial symmetry, which agrees with the available results. In the second part of the paper, applying the WKB method, we analyze the stability of a tube whose stiffness varies slowly in space in such a way that there is a "weakened" region of finite length in which the "fluid–tube" system is locally unstable. We prove that the tube is globally unstable if the local instability is absolute; otherwise, the local instability is suppressed by the surrounding locally stable regions. Solving numerically the eigenvalue problem, we demonstrate the high accuracy of the result obtained by the WKB method even for a sufficiently fast variation of stiffness along the tube axis.

DOI: 10.1134/S0081543818010030

1. INTRODUCTION

It is well known that the loss of stability and vibrations of the walls of vessels in humans and animals (blood vessels, bile ducts, ureters, and so on) play an important role in biology. In some cases, such vibrations may cause premature ageing of vessel walls; in other cases, they are significant in controlling the biofluid flow rate and pressure drop [34, 32]. For this reason, the flutter of elastic tubes conveying a fluid has been intensively studied over the last few decades [31, 15, 17].

The bending instability of elastic tubes conveying a fluid has been theoretically and experimentally investigated in many studies [30, 14]. Such instability may arise in various industrial cooling systems, including those of nuclear reactors. However, there are no data on bending instability in biological applications; apparently, bending vibrations are rapidly damped due to the effect of the tissues surrounding the vessels. Therefore, in biomechanics it is of primary interest to consider instability modes that are not accompanied by bending of the tube axis.

There are a lot of published experimental data on such instabilities in setups of the Starling resistor type [5, 6]. The observed oscillations are always associated with the collapse of the tube: the transmural pressure (difference between the external and internal pressures) in an unstable state is always negative, at least along a part of a tube. At the beginning of a cycle of oscillations, when the flow rate is high and the transmural pressure is negative, the tube is partially constricted, which increases its resistance. This slows down the flow and increases the transmural pressure. As a result,

[a] Steklov Mathematical Institute of Russian Academy of Sciences, ul. Gubkina 8, Moscow, 119991 Russia.
[b] Institute of Mechanics, Moscow State University, Michurinskii pr. 1, Moscow, 119192 Russia.
E-mail addresses: vasily@vedeneev.ru (V.V. Vedeneev), poroshina@imec.msu.ru (A.B. Poroshina).

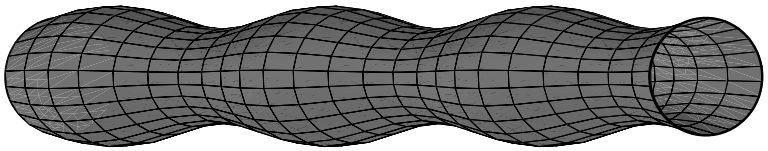

Fig. 1. Axially symmetric perturbation of an elastic tube.

the tube inflates, the flow rate increases, and the transmural pressure decreases, which completes the cycle of oscillations. During each constriction of the tube, it changes its geometrical shape and looses axial symmetry, and the flow in it remains rather complex and, as a rule, separated.

The simplest theoretical models used in the analysis of elastic tubes were first proposed in [20]; they are one-dimensional. To take into account the constriction (collapse) of tubes, one characterizes each tube by the relation between the cross section area and the transmural pressure; this relation is known as the tube law. In order to achieve a better correspondence between the one-dimensional models and the real behavior of a fluid in tubes, one includes in these models the pressure loss due to partial flow separation after the constricted region; as shown in [19, 18], this phenomenon plays an important role. A significant development of one-dimensional models that gives results in a qualitative agreement with three-dimensional numerical simulations was presented in [38]. Higher dimensional models were used in analytical and numerical investigations of the motion of a fluid and a tube on the basis of two-dimensional models [26, 25, 23] and in numerical studies based on three-dimensional models [27, 16]. However, one-dimensional models are still the main tool of simulation in hemodynamics [1, 11, 35, 33, 8, 37, 3].

Note that previously only Newtonian flows in elastic tubes have been considered in the literature. However, it is known that blood in small vessels [29, 21, 13, 2, 12] and bile [10, 22] may exhibit strong non-Newtonian properties. For example, the parameters of blood of the cardiac cycle presented in [36] are equivalent to $n = 1/8$ in the power-law rheological law. In this connection, a question arises as to whether other types of stability loss are possible that do not occur in Newtonian flows in a tube.

To investigate the effect of rheology, in this paper we study the flutter of elastic tubes conveying a power-law fluid. We use a one-dimensional model and consider axially symmetric perturbations of a tube (Fig. 1); i.e., we assume that the transmural pressure is positive. We show that although such perturbations decay in the case of a Newtonian fluid (which corresponds to the available experimental data), they may grow in the case of a small power-law index n of the medium. This means that for pseudoplastic fluids instability can be observed for positive transmural pressures, i.e., in the case when the tube does not collapse during the oscillation cycle. We also study the type of instability (absolute/convective). To analyze the problem of stability of an infinite nonuniform tube that is locally stable everywhere except for a "weakened" region with local instability, we apply the WKB method. We show that for the tube to be globally unstable, the local instability in the weakened region should be absolute.

2. DERIVATION OF SPATIALLY ONE-DIMENSIONAL EQUATIONS

2.1. Three-dimensional equations of motion of a non-Newtonian fluid. Consider a cylindrical elastic tube with a non-Newtonian power-law fluid flowing in it.

The system of equations of motion of the fluid is given by

$$\operatorname{div}\vec{v} = 0,$$

$$\frac{dv^i}{dt} = -\frac{1}{\rho}\nabla^i p + \frac{1}{\rho}\nabla_j \tau^{ij}, \qquad i = 1, 2, 3,$$

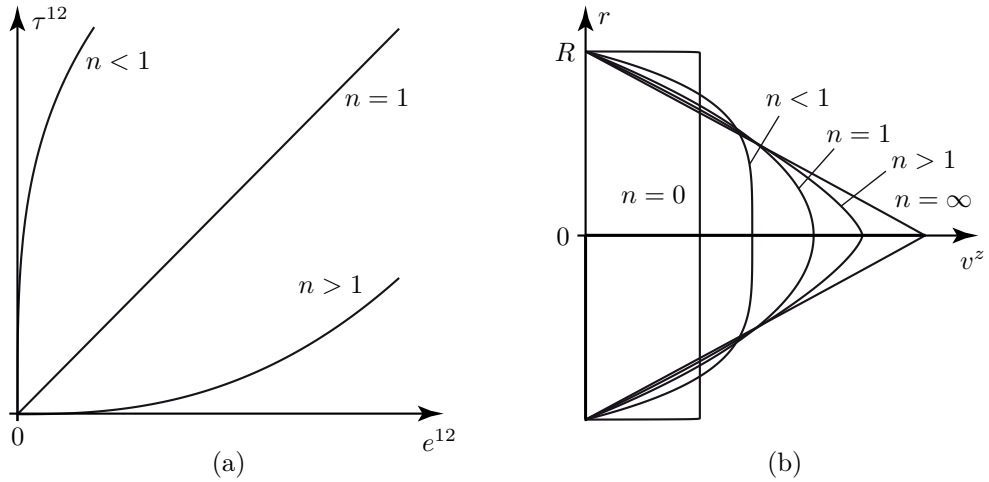

Fig. 2. (a) Power law (2.1) for pure shear. (b) Velocity profile for the Poiseuille flow.

where τ^{ij} is the viscous stress tensor. The rheology of a power-law fluid is described by the relation

$$\tau^{ij} = 2\mu\big(\sqrt{2}I_2(e)\big)^{n-1}e^{ij}, \qquad I_2(e) = \sqrt{e^{ij}e_{ij}}, \tag{2.1}$$

where e^{ij} is the strain rate tensor. This relation generalizes the simple expression for pure shear

$$\tau^{12} = \mu\left(\frac{dv_1}{dx_2}\right)^n.$$

For a Newtonian fluid, $n = 1$. The case of $0 < n < 1$ corresponds to pseudoplastic media, whose viscosity is higher for lower shear rate, and the case of $n > 1$ corresponds to dilatant media, whose viscosity increases with increasing shear rate (Fig. 2a).

Introduce a cylindrical system of coordinates with the z-axis directed along the symmetry axis of the tube and consider axially symmetric flows. Then the system of equations takes the form

$$\frac{\partial v^r}{\partial r} + \frac{\partial v^z}{\partial z} + \frac{v^r}{r} = 0, \tag{2.2}$$

$$\begin{aligned}\frac{dv^r}{dt} &= -\frac{1}{\rho}\frac{\partial p}{\partial r}\\ &+ \frac{2^{\frac{n-1}{2}}}{\rho}\left[\frac{\partial}{\partial r}\left(2\mu I_2^{n-1}\frac{\partial v^r}{\partial r}\right) - 2r\mu I_2^{n-1}\frac{1}{r^3}v^r + \frac{2}{r}\mu I_2^{n-1}\frac{\partial v^r}{\partial r} + \frac{\partial}{\partial z}\left(\mu I_2^{n-1}\left(\frac{\partial v^z}{\partial r} + \frac{\partial v^r}{\partial z}\right)\right)\right],\end{aligned} \tag{2.3}$$

$$\begin{aligned}\frac{dv^z}{dt} &= -\frac{1}{\rho}\frac{\partial p}{\partial z}\\ &+ \frac{2^{\frac{n-1}{2}}}{\rho}\left[\frac{\partial}{\partial r}\left(\mu I_2^{n-1}\left(\frac{\partial v^z}{\partial r} + \frac{\partial v^r}{\partial z}\right)\right) + \frac{\mu}{r}I_2^{n-1}\left(\frac{\partial v^z}{\partial r} + \frac{\partial v^r}{\partial z}\right) + \frac{\partial}{\partial z}\left(2\mu I_2^{n-1}\frac{\partial v^z}{\partial z}\right)\right].\end{aligned} \tag{2.4}$$

For a steady flow in a rigid cylindrical tube of constant radius R_0, a solution to system (2.2)–(2.4) is given by the Poiseuille velocity profile

$$v^r = 0, \qquad v^z(r) = 2^{-\frac{1}{n}}\left(\frac{k}{\mu}\right)^{\frac{1}{n}}\frac{n}{n+1}\left(R_0^{\frac{n+1}{n}} - r^{\frac{n+1}{n}}\right), \qquad \frac{\partial p}{\partial z} = -k = \text{const}. \tag{2.5}$$

Velocity profiles for various n are shown in Fig. 2b. For a Newtonian fluid ($n = 1$), we obtain the standard parabolic velocity profile.

2.2. Assumptions. We will assume that the tube is deformed in such a way that every cross section $S(z,t)$ of the tube remains circular and the points of the tube move only radially (Fig. 1). Then the position of the tube is defined by the cross section radius of the tube $R(z,t)$ at the point z at time t. The interaction between the medium and the tube occurs due to the no-slip condition and the equality of normal stresses. We neglect the longitudinal displacements. To simplify the two-dimensional system (2.2)–(2.4) to a one-dimensional system of equations in terms of the cross section radius R and the flow rate Q, we integrate each equation over the cross section while taking into account the interaction between the fluid and the tube.

We assume that the perturbations

(1) have wavelength much greater than the radius R;

(2) have low oscillation frequency, so that the flow can be assumed to be quasisteady.

Under these conditions, the relative velocity $V(\xi,z,t) = v^z(r,z,t)/v_{\mathrm{av}}(z,t)$ (where $\xi = r/R$ and $v_{\mathrm{av}}(z,t) = Q/(\pi R^2)$ is the average velocity) is independent of the cross section radius $R(z,t)$ and the local flow rate $Q(z,t)$.

Calculating the average velocity for the profile (2.5), we find

$$V(\xi,z,t) = \frac{1+3n}{1+n}\Big(1-\xi^{\frac{n+1}{n}}\Big).$$

Hence,

$$v^z(r,z,t) = \frac{Q(z,t)}{\pi R^2(z,t)}\,\frac{1+3n}{1+n}\left(1-\left(\frac{r}{R}\right)^{\frac{n+1}{n}}\right). \tag{2.6}$$

2.3. Averaging the system of equations over the cross section. Integrating the continuity equation (2.2) over the cross section, we obtain the first equation of the one-dimensional problem:

$$\frac{\partial Q}{\partial z} + \pi\frac{\partial R^2(z,t)}{\partial t} = 0. \tag{2.7}$$

To derive the second one-dimensional equation, we integrate equation (2.4), which takes the form

$$\int\limits_{S(z,t)}\left(\frac{\partial v^z}{\partial t} + v^r\frac{\partial v^z}{\partial r} + v^z\frac{\partial v^z}{\partial z}\right)dS = -\int\limits_{S(z,t)}\frac{1}{\rho}\frac{\partial p}{\partial z}\,dS$$
$$+\frac{2^{\frac{n-1}{2}}}{\rho}\int\limits_{S(z,t)}\left[\frac{\partial}{\partial r}\left(\mu I_2^{n-1}\left(\frac{\partial v^z}{\partial r}+\frac{\partial v^r}{\partial z}\right)\right)+\frac{\mu}{r}I_2^{n-1}\left(\frac{\partial v^z}{\partial r}+\frac{\partial v^r}{\partial z}\right)+\frac{\partial}{\partial z}\left(2\mu I_2^{n-1}\frac{\partial v^z}{\partial z}\right)\right]dS.$$

Then we transform it as follows.

First, using the continuity equation $\partial v^z/\partial z = -(1/r)\partial(rv^r)/\partial r$ and the no-slip condition $v^z(R,z,t) = 0$ on the tube walls, by integration by parts we obtain

$$\int\limits_{S(z,t)} v^r\frac{\partial v^z}{\partial r}\,dS = 2\pi\int\limits_0^R rv^r\frac{\partial v^z}{\partial r}\,dr = -2\pi\int\limits_0^R v^z\left(-r\frac{\partial v^z}{\partial z}\right)dr = \int\limits_{S(z,t)} v^z\frac{\partial v^z}{\partial z}\,dS.$$

Using the velocity profile (2.6), after several transformations, we obtain

$$\int\limits_{S(z,t)} v^z\frac{\partial v^z}{\partial z}\,dS = \frac{1}{2}\frac{\partial}{\partial z}\left(\frac{(3n+1)Q(z,t)^2}{(2n+1)\pi R(z,t)^2}\right).$$

Second, we rewrite the term containing pressure as follows:

$$\int\limits_{S(z,t)} \frac{1}{\rho}\frac{\partial p}{\partial z}\,dS = \frac{\pi R(z,t)^2}{\rho}\frac{\partial P(z,t)}{\partial z},$$

where

$$P(z,t) = \frac{1}{\pi R^2(z,t)} \int\limits_{S(z,t)} p(r,z,t)\,dS$$

is the mean pressure in the cross section.

Finally, we transform the viscous terms on the right-hand side as follows. The first two terms have the form

$$\begin{aligned}\frac{2^{\frac{n+1}{2}}\pi}{\rho}\int\limits_0^R r\left(\frac{\partial}{\partial r}\left(\mu I_2^{n-1}\left(\frac{\partial v^z}{\partial r}+\frac{\partial v^r}{\partial z}\right)\right)+\frac{1}{r}\mu I_2^{n-1}\left(\frac{\partial v^z}{\partial r}+\frac{\partial v^r}{\partial z}\right)\right)dr&\\ = \frac{2^{\frac{n+1}{2}}\pi}{\rho}\int\limits_0^R \frac{\partial}{\partial r}\left(r\mu I_2^{n-1}\left(\frac{\partial v^z}{\partial r}+\frac{\partial v^r}{\partial z}\right)\right)dr&\\ = \frac{2^{\frac{n+1}{2}}\pi R(z,t)}{\rho}\mu I_2^{n-1}\left(\frac{\partial v^z}{\partial r}+\frac{\partial v^r}{\partial z}\right)(R(z,t),z,t).&\end{aligned}$$

For further transformations, we should take into consideration the long-wavelength approximation, i.e., the fact that the characteristic ratio of the radius to the length, R/L, is a small parameter ε. It follows from the continuity equation that the radial and longitudinal velocities are estimated as $v^r/v^z \sim R/L \sim \varepsilon$. Then

$$\mu I_2^{n-1}\left(\frac{\partial v^z}{\partial r}+\frac{\partial v^r}{\partial z}\right) = \mu\left(\frac{1}{2}\left(\frac{\partial v^z}{\partial r}\right)^2+O(\varepsilon^2)\right)^{\frac{n-1}{2}}\left(\frac{\partial v^z}{\partial r}+\frac{\partial v^r}{\partial z}\right) = -\mu 2^{\frac{1-n}{2}}\left|\frac{\partial v^z}{\partial r}\right|^n + O(\varepsilon^2).$$

From the expression (2.6) for velocity we find

$$\frac{\partial v^z}{\partial r}(r,z,t) = -\frac{Q}{\pi R^2(z,t)}\frac{3n+1}{n}\frac{r^{\frac{1}{n}}}{R(z,t)^{\frac{n+1}{n}}}.$$

Then

$$\frac{2^{\frac{n+1}{2}}\pi R(z,t)}{\rho}\mu I_2^{n-1}\left(\frac{\partial v^z}{\partial r}+\frac{\partial v^r}{\partial z}\right)\Big|_{r=R} = -\frac{\mu}{\rho}\frac{2(3n+1)^n Q^n r}{n^n\pi^{n-1}R(z,t)^{3n}}\Big|_{r=R} = -\frac{\mu}{\rho}\frac{2(3n+1)^n Q^n}{n^n\pi^{n-1}R(z,t)^{3n-1}}.$$

The last viscous term

$$\frac{2^{\frac{n-1}{2}}}{\rho}\int\limits_S \frac{\partial}{\partial z}\left(2\mu I_2^{n-1}\frac{\partial v^z}{\partial z}\right)dS$$

is of order ε^2 and can be neglected.

As a result, equation (2.4) integrated over the cross section takes the form

$$\frac{\partial Q(z,t)}{\partial t}+\frac{\partial}{\partial z}\left(\frac{(3n+1)Q(z,t)^2}{(2n+1)\pi R(z,t)^2}\right)+\frac{\mu}{\rho}\frac{2(3n+1)^n Q(z,t)^n}{n^n\pi^{n-1}R(z,t)^{3n-1}}+\frac{\pi R(z,t)^2}{\rho}\frac{\partial P(z,t)}{\partial z}=0. \qquad (2.8)$$

2.4. Model of a tube. To derive the last equation, we should relate the fluid pressure to the motion of the tube wall. For simplicity, we will neglect the mass of the tube and its tension and take into account only the elastic force caused by the variation of the radius:

$$\beta(R - R_0) = P, \tag{2.9}$$

where

$$\beta = \frac{Eh}{(1-\nu^2)R_0^2}$$

is the radial stiffness of the tube, R_0 is the radius of the undeformed tube, E and ν are the Young's modulus and the Poisson coefficient, and h is the tube wall thickness.

2.5. One-dimensional system of equations. So, the closed system of equations (2.7)–(2.9) for the three unknowns Q, R, and P in the variables z and t has the form

$$\frac{\partial Q}{\partial z} + \frac{\partial(\pi R^2)}{\partial t} = 0, \tag{2.10}$$

$$\frac{\partial Q}{\partial t} + \frac{\partial}{\partial z}\left(\frac{(3n+1)Q^2}{(2n+1)\pi R^2}\right) + \frac{\mu}{\rho}\frac{2(3n+1)^n Q^n}{n^n \pi^{n-1} R^{3n-1}} + \frac{\pi R^2}{\rho}\frac{\partial P}{\partial z} = 0, \tag{2.11}$$

$$\beta(R - R_0) = P. \tag{2.12}$$

This system was first obtained in [39] in somewhat different terms.

2.6. Comparison with other one-dimensional models. Equation (2.10) has the standard form of a one-dimensional continuity equation [15]. The equation of motion of the tube (2.12) also has the standard form; however, in contrast to other studies, we do not take account of the "tube law" for negative transmural pressures: this law is needed to determine oscillations related to the collapse of a part of the tube; however, the goal of the present work is to study oscillations for positive transmural pressures, which are not accompanied by a collapse of the tube.

The momentum equation (2.11) is more complicated, and we need to do some additional work to analyze it. As a rule [15], a one-dimensional momentum equation is expressed in the standard form

$$\rho\left(\frac{\partial v}{\partial t} + v\frac{\partial v}{\partial z}\right) = -\frac{dp}{dz} - F, \tag{2.13}$$

where $v(z,t)$ and $p(z,t)$ are the average longitudinal velocity and pressure of the fluid and F is a term in which the friction losses are taken into account. Multiplying equation (2.11) by $\rho/(\pi R^2)$, we can rewrite it in a similar form

$$\rho\left(\frac{1}{\pi R^2}\frac{\partial Q}{\partial t} + \frac{1}{\pi R^2}\frac{\partial}{\partial z}\left(\frac{(3n+1)Q^2}{(2n+1)\pi R^2}\right)\right) = -\frac{\partial P}{\partial z} - \mu\frac{2(3n+1)^n Q^n}{n^n \pi^n R^{3n+1}}. \tag{2.14}$$

When one writes the left-hand side of equation (2.13), one assumes a uniform velocity distribution, i.e., neglects the Poiseuille velocity distribution. This is equivalent to the case of $n = 0$, because in this situation the velocity profile is uniform (Fig. 2b). For $n = 0$, introducing the average velocity $v = Q(z,t)/(\pi R^2)$ and applying the continuity equation, we transform the left-hand side of equation (2.14) into

$$\rho\left(\frac{\partial v}{\partial t} + v\frac{\partial v}{\partial z}\right),$$

which coincides with the left-hand side of (2.13). It is clear that for $n \neq 0$ the left-hand side of equation (2.14) reflects the effect of the Poiseuille velocity distribution on the integral convective

derivative. A similar form of the right-hand side of the momentum equation was used for $n \neq 0$ in [36, 11].

Finally, consider the term that describes the viscous pressure losses:

$$\mu \frac{2(3n+1)^n Q^n}{n^n \pi^n R^{3n+1}}. \tag{2.15}$$

For $n = 1$, this term takes the form

$$\mu \frac{8Q}{\pi R^4}, \tag{2.16}$$

which is the pressure loss in an ordinary Newtonian flow with the Poiseuille velocity distribution. For example, in this form the term F was taken in [20]. It is clear that for $n \neq 1$ the expression (2.15) is a generalization of the term responsible for viscous losses to power-law fluids.

A similar one-dimensional model was used in [36, 11] for designing a model of a blood vessel network. However, taking account of the velocity profile (2.5) and obtaining the same convective term as the second term in (2.11), the authors of these studies took the viscous pressure losses in the form (2.16); i.e., they neglected the non-Newtonian rheology.

2.7. Transition to dimensionless variables. As dimensionally independent quantities, we take the fluid density ρ, the tube radius R_0, and the flow rate Q_0 at the inlet of the tube. Then the other quantities can be nondimensionalized as follows:

$$R = R_0 \widetilde{R}, \qquad Q = Q_0 \widetilde{Q}, \qquad P = \frac{\rho_0 Q_0^2}{R_0^4} \widetilde{P}, \qquad \beta = \frac{\rho_0 Q_0^2}{R_0^5} \widetilde{\beta}, \qquad z = R_0 \widetilde{z}, \qquad t = \frac{R_0^3}{Q_0} \widetilde{t},$$

where the variables with tildes are dimensionless.

The viscosity of the fluid is nondimensionalized through the Reynolds number, which is introduced for power-law fluids in tubes as in [28]:

$$\mathsf{Re} = \frac{\rho (2R_0)^n v_{\mathrm{av}}^{2-n}}{8^{n-1} \mu \left(\frac{3n+1}{4n}\right)^n} = \frac{\rho R_0^n v_{\mathrm{av}}^{2-n}}{\mu} \frac{8n^n}{(3n+1)^n}.$$

Expressing the average velocity as $v_{\mathrm{av}} = Q_0/(\pi R_0^2)$, we obtain

$$\mu = \frac{\rho Q_0^{2-n}}{R_0^{4-3n}} \frac{\pi^{n-2}}{\mathsf{Re}} \frac{8n^n}{(3n+1)^n}.$$

As a result, system (2.10)–(2.12) takes the following dimensionless form:

$$\frac{\partial \widetilde{Q}}{\partial \widetilde{z}} + \frac{\partial (\pi \widetilde{R}^2)}{\partial \widetilde{t}} = 0, \tag{2.17}$$

$$\frac{\partial \widetilde{Q}}{\partial \widetilde{t}} + \frac{\partial}{\partial \widetilde{z}} \left(\frac{(3n+1)\widetilde{Q}^2}{(2n+1)\pi \widetilde{R}^2} \right) + \frac{16 \widetilde{Q}^n}{\pi\, \mathsf{Re}\, \widetilde{R}^{3n-1}} + \pi \widetilde{R}^2 \frac{\partial \widetilde{P}}{\partial \widetilde{z}} = 0, \tag{2.18}$$

$$\widetilde{\beta}(\widetilde{R} - 1) = \widetilde{P}. \tag{2.19}$$

Substituting the value of P expressed in terms of R from (2.19) into (2.18) and omitting the tildes, we finally obtain a dimensionless system of two spatially one-dimensional equations

$$\frac{\partial Q}{\partial z} + \frac{\partial (\pi R^2)}{\partial t} = 0, \tag{2.20}$$

$$\frac{\partial Q}{\partial t} + \frac{\partial}{\partial z} \left(\frac{(3n+1)Q^2}{(2n+1)\pi R^2} \right) + \frac{16 Q^n}{\pi\, \mathsf{Re}\, R^{3n-1}} + \pi R^2 \beta \frac{\partial R}{\partial z} = 0. \tag{2.21}$$

3. LOCAL STABILITY CHARACTERISTICS

3.1. Equations for perturbations. Consider a steady state with the flow rate $Q = 1$ and tube radius $R = R_{\mathrm{s}}(z)$. Perturbations of the steady state have the form

$$Q = 1 + Q'(z,t), \qquad R = R_{\mathrm{s}}(z) + R'(z,t).$$

Let us substitute these expressions into system (2.20), (2.21) and linearize it. After a series of algebraic transformations, the linearized system of equations for perturbations takes the form

$$\frac{\partial Q'(z,t)}{\partial z} + 2\pi R_{\mathrm{s}} \frac{\partial R'(z,t)}{\partial t} = 0, \tag{3.1}$$

$$\begin{aligned}\frac{\partial Q'(z,t)}{\partial t} + \frac{2(3n+1)}{(2n+1)\pi R_{\mathrm{s}}(z)^2}\frac{\partial Q'(z,t)}{\partial z} + \left[\frac{16n}{\pi\,\mathsf{Re}\,R_{\mathrm{s}}^{3n-1}(z)} - \frac{4(3n+1)}{(2n+1)\pi R_{\mathrm{s}}^3(z)}\frac{\partial R_{\mathrm{s}}(z)}{\partial z}\right]Q'(z,t)\\ + \left[\left(2\pi\beta R_{\mathrm{s}}(z) + \frac{6(3n+1)}{(2n+1)\pi R_{\mathrm{s}}^4}\right)\frac{\partial R_{\mathrm{s}}(z)}{\partial z} + \frac{16(1-3n)}{\pi\,\mathsf{Re}\,R_{\mathrm{s}}^{3n}(z)}\right]R'(z,t)\\ + \left[\pi\beta R_{\mathrm{s}}^2(z) - \frac{2(3n+1)}{\pi(2n+1)R_{\mathrm{s}}^3(z)}\right]\frac{\partial R'(z,t)}{\partial z} = 0.\end{aligned} \tag{3.2}$$

3.2. Dispersion equation. First, we analyze the local stability of the tube. Suppose that $\lambda \ll L$, where λ is the wavelength; i.e., we will consider waves with wavelength much less than the distance at which the tube radius is significantly changed, which allows us to set $R_{\mathrm{s}} = \mathrm{const}$. Then equation (3.2) becomes an equation with constant coefficients and admits a solution in the form of traveling waves. On the other hand, equation (3.2) is derived under the condition $\lambda \gg R$, so we assume that both inequalities

$$R \ll \lambda \ll L \tag{3.3}$$

are satisfied.

Taking the local value of R_{s} as the length scale R_0 and renormalizing the other variables, we assume without loss of generality that $R_{\mathrm{s}} \equiv 1$ and consider solutions in the form of traveling waves $Q' = \widehat{Q}e^{i(kz-\omega t)}$ and $R' = \widehat{R}e^{i(kz-\omega t)}$. Equation (3.1) reduces to

$$\widehat{Q}ke^{i(kz-\omega t)} + 2\pi(-\omega)\widehat{R}e^{i(kz-\omega t)} = 0 \qquad \Rightarrow \qquad \widehat{R} = \frac{\widehat{Q}k}{2\pi\omega}.$$

Equation (3.2) turns into

$$\begin{aligned}-\widehat{Q}\omega i e^{i(kz-\omega t)} + \frac{2(3n+1)}{(2n+1)\pi}ki\widehat{Q}e^{i(kz-\omega t)} + \frac{16n}{\pi\,\mathsf{Re}}\widehat{Q}e^{i(kz-\omega t)} + \frac{16(1-3n)}{\pi\,\mathsf{Re}}\widehat{R}e^{i(kz-\omega t)}\\ + \left(\pi\beta - \frac{2(3n+1)}{\pi(2n+1)}\right)\widehat{R}kie^{i(kz-\omega t)} = 0.\end{aligned}$$

Substituting the expression for $\widehat{R}$ into this relation and dividing the result by $\widehat{Q}e^{i(kz-\omega t)}$, we obtain the dispersion relation

$$\omega^2 + \left(\frac{16n}{\pi\,\mathsf{Re}}i - \frac{2(3n+1)k}{\pi(2n+1)}\right)\omega + \frac{8(1-3n)k}{\pi^2\,\mathsf{Re}}i - \frac{k^2\beta}{2} + \frac{k^2(3n+1)}{\pi^2(2n+1)} = 0. \tag{3.4}$$

Since this is a quadratic equation in ω, its discriminant is given by

$$D = -\frac{(16n)^2}{\pi^2\,\mathsf{Re}^2} + 2k^2\beta - \frac{32(n+1)k}{\pi^2\,\mathsf{Re}(2n+1)}i + \frac{4(3n+1)nk^2}{(2n+1)^2\pi^2} \tag{3.5}$$

and the roots are

$$\omega_{1,2}(k) = \frac{2}{2+mk^2}\left[\frac{(3n+1)k}{(2n+1)\pi} - \frac{8n}{\pi\,\mathsf{Re}}i \pm \frac{1}{2}\sqrt{D}\right]. \tag{3.6}$$

It follows from (3.6) that one branch of ω always has a negative imaginary part. Thus, one of the waves for each k always decays, and only one wave may grow and lead to instability.

3.3. Stability criterion. A wave is growing if $\operatorname{Im}\omega(k) > 0$. The value of $\operatorname{Im}\omega(k)$ can be found from (3.6), with the root calculated explicitly by the formula $\sqrt{a+ib} = \alpha + i\gamma$ where

$$\gamma = \pm\frac{b}{\sqrt{2}\sqrt{a+\sqrt{a^2+b^2}}}.$$

The calculations yield

$$\operatorname{Im}\omega = -\frac{8n}{\pi\,\mathsf{Re}} \pm \frac{16k(n+1)}{\sqrt{2}\pi^2\,\mathsf{Re}\,(2n+1)}\left[2k^2\left(\beta + \frac{2(3n+1)n}{(2n+1)^2\pi^2}\right) - \frac{(16n)^2}{\pi^2\,\mathsf{Re}^2} + \left\{\frac{32^2k^2(n+1)^2}{\pi^4\,\mathsf{Re}^2(2n+1)^2}\right.\right.$$
$$\left.\left. + 4k^4\left(\beta + \frac{2(3n+1)n}{(2n+1)^2\pi^2}\right)^2 - 4k^2\left(\beta + \frac{2(3n+1)n}{(2n+1)^2\pi^2}\right)\frac{(16n)^2}{\pi^2\,\mathsf{Re}^2} + \frac{(16n)^4}{\pi^4\,\mathsf{Re}^4}\right\}^{\frac{1}{2}}\right]^{-\frac{1}{2}}. \tag{3.7}$$

Eliminating the square roots by squaring, we reduce the inequality $\operatorname{Im}\omega > 0$ to

$$\frac{8(n+1)^2}{\pi^2(2n+1)^2n^2}\left(\frac{-(6n^3-n^2-1)}{2n^2\pi^2(2n+1)} - \beta\right)k^4 > 0.$$

Here one can see that, first, the sign of $\operatorname{Im}\omega(k)$ cannot change for nonzero k, so all waves either decay or grow. Second, the instability criterion $\operatorname{Im}\omega > 0$ reduces to the following inequality:

$$\beta < \beta_{\mathrm{fl}}(n) = \frac{-(6n^3-n^2-1)}{2n^2\pi^2(2n+1)}. \tag{3.8}$$

Since $\beta > 0$, instability can arise only when the right-hand side is positive. This is the case when

$$n < 0.611.$$

The instability domain $\beta < \beta_{\mathrm{fl}}(n)$ is shown in Fig. 3.

Note that the instability criterion is independent of the Reynolds number Re, which determines the absolute values of the growth rates of the waves but not their sign. One can also notice that axially symmetric instability is possible only for pseudoplastic fluids; in particular, instability modes of Newtonian flows in elastic tubes can only be non-axisymmetric, which is confirmed by all the available experimental data.

3.4. Absolute and convective instability. Even if the tube conveying a pseudoplastic fluid is unstable, this instability may not be observed in reality when the instability is convective. In this case, the localized perturbations grow but are simultaneously carried downstream by the flow and can leave a given domain while having a small amplitude. If the instability is absolute, then the localized perturbations grow so that the domain occupied by them expands both downstream and upstream. The absolute instability criterion is given in [7, 4]; it consists of two conditions:

(1) there exists a saddle point ω_{s} of the function $\omega(k)$ in the upper half-plane of the complex plane ω; i.e., $d\omega/dk = 0$ for $\omega = \omega_{\mathrm{s}}$ and $\operatorname{Im}\omega_{\mathrm{s}} > 0$;

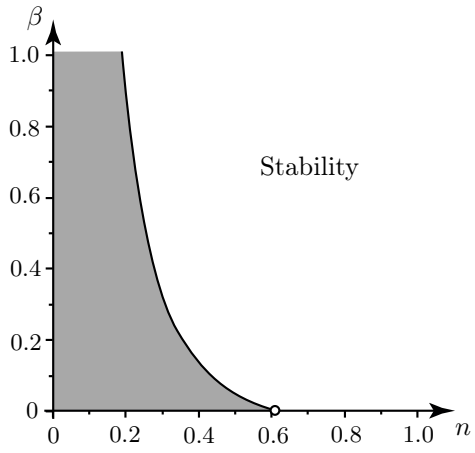

Fig. 3. Instability domain.

(2) the inverse function $k(\omega)$ has a branch point at ω_{s}. The branches $k_1(\omega_{\mathrm{s}}) = k_2(\omega_{\mathrm{s}})$ that merge at this point should correspond to waves traveling in opposite directions; i.e., $\operatorname{Im} k_1(\omega) \to +\infty$ and $\operatorname{Im} k_2(\omega) \to -\infty$ as $\operatorname{Im}\omega \to +\infty$, or vice versa.

For the problem on the behavior of localized perturbations to be well-posed, it is necessary that the short waves decay, i.e., $\operatorname{Im}\omega(k) < 0$ as $k \to \pm\infty$ along the real k-axis. It can be shown that one can make this condition valid by taking into account the weak inertia of the tube. Assume that the mass of the tube is small; therefore, the corresponding terms are needed only to stabilize the short waves and can be neglected in the analysis of the branch point.

To obtain an absolute instability criterion, it is convenient to rewrite the left-hand side of the dispersion relation (3.4) as a polynomial in k:

$$\left(\frac{3n+1}{\pi^2(2n+1)} - \frac{\beta}{2}\right)k^2 + \left(\frac{8(1-3n)}{\pi^2\,\mathsf{Re}}i - \frac{2(3n+1)}{\pi(2n+1)}\omega\right)k + \left(\omega^2 + \frac{16n}{\pi\,\mathsf{Re}}i\omega\right) = 0. \tag{3.9}$$

This is a quadratic equation in $k(\omega)$; hence, there exist two spatial branches. The branch points ω_{s} of the function $k(\omega)$ are determined from the condition of vanishing discriminant. By straightforward transformations, we again obtain a quadratic equation for ω_{s}:

$$\begin{aligned} D_k = {} & 4\left(\frac{(3n+1)^2}{\pi^2(2n+1)^2} - \frac{3n+1}{\pi^2(2n+1)} + \frac{\beta}{2}\right)\omega^2 \\ & - 4\left(\frac{8(3n+1)(1-3n)}{\pi^3\,\mathsf{Re}(2n+1)} + \left(\frac{3n+1}{\pi^2(2n+1)} - \frac{\beta}{2}\right)\frac{16n}{\pi\,\mathsf{Re}}\right)i\omega - \frac{8^2(1-3n)^2}{\pi^4\,\mathsf{Re}^2} = 0. \end{aligned} \tag{3.10}$$

Using equation (3.10), one can easily show that the condition $\operatorname{Im}\omega_{\mathrm{s}} > 0$ is satisfied if and only if the expression in parentheses in the second term is positive, i.e.,

$$\frac{(3n+1)(1-3n)}{2n(2n+1)} + \frac{3n+1}{2n+1} - \frac{\pi^2\beta}{2} > 0.$$

This inequality can be rewritten as

$$\beta < \beta_{\mathrm{abs}}(n) = \frac{(3n+1)(1-n)}{\pi^2 n(2n+1)}. \tag{3.11}$$

Condition (3.11) shows that the saddle point ω_{s} of $\omega(k)$ with $\operatorname{Im}\omega_{\mathrm{s}} > 0$ exists only for sufficiently soft tubes.

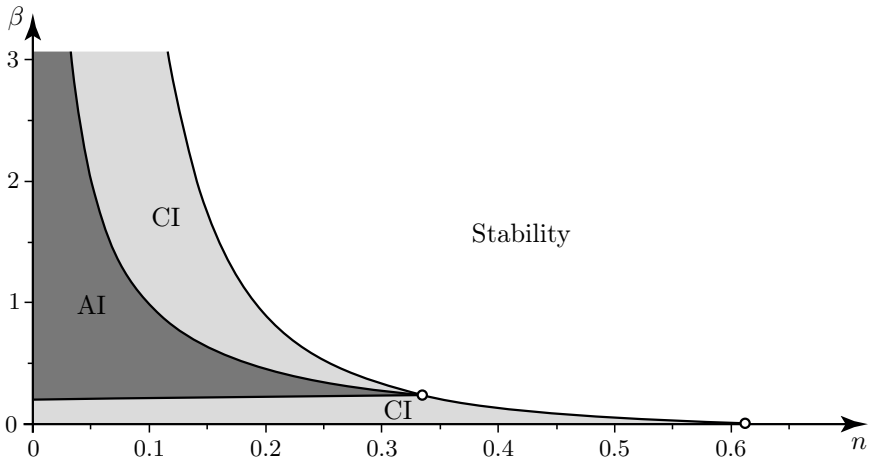

Fig. 4. Domains of absolute (AI) and convective (CI) instability.

Further, consider the second condition of absolute instability, namely, the wave propagation direction. The solutions $k(\omega)$ to the dispersion equation (3.9) for $|\omega| \to \infty$ have the form

$$k_{1,2} = \left(\frac{3n+1}{\pi^2(2n+1)} - \frac{\beta}{2}\right)^{-1}\left(\frac{3n+1}{\pi(2n+1)} \pm \sqrt{\left(\frac{3n+1}{\pi(2n+1)}\right)^2 - \left(\frac{3n+1}{\pi^2(2n+1)} - \frac{\beta}{2}\right)}\right)\omega.$$

It is easy to see that the spatial waves propagate in opposite directions if

$$\frac{3n+1}{\pi^2(2n+1)} - \frac{\beta}{2} < 0 \qquad \Rightarrow \qquad \beta > \beta_{\mathrm{div}} = \frac{2(3n+1)}{\pi^2(2n+1)}. \tag{3.12}$$

As a result, the criterion of absolute instability is given by the inequalities

$$\beta_{\mathrm{div}}(n) < \beta < \beta_{\mathrm{abs}}(n). \tag{3.13}$$

This condition may hold only for $n < 1/3$ since the three curves $\beta_{\mathrm{div}}(n)$, $\beta_{\mathrm{abs}}(n)$, and $\beta_{\mathrm{fl}}(n)$ intersect at the point $n = 1/3$. The domain of absolute instability is shown in Fig. 4.

Note that the domains of convective instability that surround the domain of absolute instability in Fig. 4 are different. The domain below the domain of absolute instability is formed by parameters for which both waves propagate downstream, so any perturbation is also carried downstream and leaves a finite domain in finite time. A saddle point of $\omega(k)$, although exists, has nothing to do with the asymptotics of localized perturbations of the tube. The domain of convective instability above the domain of absolute instability is formed by parameters for which one wave propagates downstream while the other propagates upstream. However, the saddle point of the function $\omega(k)$ lies in the domain $\operatorname{Im}\omega < 0$. Note also that the first domain $\{\beta < \beta_{\mathrm{div}}\}$ corresponds to very "weak" tubes: in the steady state, such tubes are not constricted due to the pressure drop but rather expand [39]. Below we do not consider these parameter values.

4. GLOBAL INSTABILITY OF A NONUNIFORM TUBE WITH A LOCALLY WEAKENED SECTION

4.1. Eigenvalue problem. Now, consider a nonuniform tube with properties varying in space. We will analyze the time-harmonic perturbations

$$\begin{pmatrix} Q'(z,t) \\ R'(z,t) \end{pmatrix} = \begin{pmatrix} Q''(z) \\ R''(z) \end{pmatrix} e^{-i\omega t}.$$

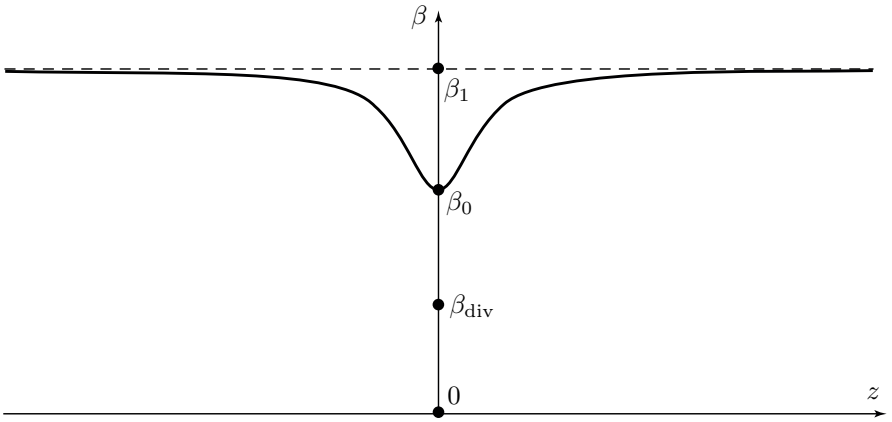

Fig. 5. Function $\beta(z)$ (4.2).

Then equation (3.1) implies

$$R'' = -\frac{i}{2\pi R_{\text{s}}\omega}\frac{dQ''}{dz}.$$

Substituting these expressions into (3.2) and combining the terms, we obtain an equation for $Q''(z)$:

$$\frac{1}{2\pi R_{\text{s}}}\left[\pi\beta R_{\text{s}}^2 - \frac{2(3n+1)}{(2n+1)\pi R_{\text{s}}^3}\right]\frac{d^2Q''}{dz^2}$$
$$+\left[\frac{1}{2\pi R_{\text{s}}}\left\{\left(2\pi\beta R_{\text{s}} + \frac{6(3n+1)}{(2n+1)\pi R_{\text{s}}^4}\right)\frac{dR_{\text{s}}}{dz} + \frac{16(1-3n)}{\pi\,\mathsf{Re}\,R_{\text{s}}^{3n}}\right\} + i\omega\frac{2(3n+1)}{(2n+1)\pi R_{\text{s}}^2}\right]\frac{dQ''}{dz}$$
$$+\left[\omega^2 + i\omega\left(\frac{16n}{\pi\,\mathsf{Re}\,R_{\text{s}}^{3n-1}} - \frac{4(3n+1)}{(2n+1)\pi R_{\text{s}}^3}\frac{dR_{\text{s}}}{dz}\right)\right]Q'' = 0, \qquad (4.1)$$

where $\beta(z)$ and $R_{\text{s}}(z)$ are fixed distributions of stiffness and the radius of the unperturbed state of the tube.

Further, assume that the tube has constant radius $R_{\text{s}}(z) \equiv \text{const} = 1$ in the unperturbed state. Such a situation occurs when the pressure drop due to viscous friction in the tube is compensated by the drop of external pressure (for example, when the tube models a vessel in a body with nonconstant external pressure). We will also assume that the stiffness of the tube is nonconstant and is given by

$$\beta(z) = \frac{\beta_0 + \beta_1(\varepsilon z)^2}{1 + (\varepsilon z)^2}. \qquad (4.2)$$

This function defines a distribution that tends to β_1 as $z \to \pm\infty$ and has a local region where the stiffness decreases to β_0 (Fig. 5). Assume that $\beta_1 > \beta_{\text{fl}}$ and $\beta_{\text{div}} < \beta_0 < \beta_{\text{fl}}$; i.e., assume that outside some interval the tube is locally stable, while in the interval it is locally unstable. The parameter ε defines the width of the "weakened" region; in what follows, we will assume that $\varepsilon \ll 1$, i.e., the stiffness of the tube varies rather slowly. This allows us to apply the WKB method in order to construct eigenfunctions.

Thus, the equation for the perturbation of the flow rate $Q''(z)$ takes the final form

$$\frac{\beta(z) - \beta_{\text{div}}}{2}\frac{d^2Q''}{dz^2} + B(\omega)\frac{dQ''}{dz} + C(\omega)Q'' = 0, \qquad (4.3)$$

where

$$B(\omega) = \frac{8(1-3n)}{\pi^2\,\mathsf{Re}} + i\omega\frac{2(3n+1)}{(2n+1)\pi}, \qquad C(\omega) = \omega^2 + i\omega\frac{16n}{\pi\,\mathsf{Re}}.$$

The problem consists in finding eigenfrequencies ω for which the corresponding eigenfunction, i.e., the solution to equation (4.3), decays at infinity, $Q''(z) \to 0$ as $z \to \pm\infty$. If one of such frequencies has positive imaginary part, $\operatorname{Im}\omega > 0$, then the system is globally unstable. In this case the local instability of the weakened region leads to the instability of the tube as a whole. Otherwise, if all eigenfunctions decay, the local instability is suppressed by the surrounding locally stable regions.

4.2. Reduction to the canonical form. The slow variation of the stiffness $\beta(z)$ allows us to apply the WKB method in order to construct the eigenfunctions of equation (4.3). For convenience, we first transform this equation by getting rid of the first derivative dQ''/dz. To this end, we make the substitution

$$\begin{aligned}\varphi(z) &= Q''(z)\exp\biggl\{\int \frac{B(\omega)}{\beta(z)-\beta_{\mathrm{div}}}\,dz\biggr\}\\ &= Q''(z)\exp\biggl\{\frac{B(\omega)}{\beta_1-\beta_{\mathrm{div}}}\biggl(z+\frac{(1-a)}{\varepsilon\sqrt{(a-d)(1-d)}}\arctan\biggl(\frac{1-d}{\sqrt{(a-d)(1-d)}}\,\varepsilon z\biggr)\biggr)\biggr\},\end{aligned} \tag{4.4}$$

where the following simplifying notation is used:

$$d=\frac{\beta_{\mathrm{div}}}{\beta_1}<a=\frac{\beta_0}{\beta_1}<1.$$

Then the function $\varphi(z)$ satisfies the equation

$$\frac{d^2\varphi}{dz^2}+p(z,\omega)\varphi=0, \tag{4.5}$$

where

$$p(z,\omega)=\frac{C(1+(\varepsilon z)^2)\bigl((\beta_0-\beta_{\mathrm{div}})+(\beta_1-\beta_{\mathrm{div}})(\varepsilon z)^2\bigr)-B^2(1+(\varepsilon z)^2)^2+2B(\beta_1-\beta_0)\varepsilon^2 z}{\bigl((\beta_0-\beta_{\mathrm{div}})+(\beta_1-\beta_{\mathrm{div}})(\varepsilon z)^2\bigr)^2}.$$

Note that the last term in the numerator is of lower order than the other terms; therefore, we can neglect it. To simplify further calculations, we introduce the notation

$$b(\omega)=\frac{B(\omega)}{\beta_0-\beta_{\mathrm{div}}},\qquad c(\omega)=\frac{C(\omega)}{\beta_0-\beta_{\mathrm{div}}},\qquad \varkappa=\frac{\beta_1-\beta_{\mathrm{div}}}{\beta_0-\beta_{\mathrm{div}}}>1.$$

Then the expression for $p(z,\omega)$ takes the form

$$p(z,\omega)=\frac{c(1+(\varepsilon z)^2)(1+\varkappa(\varepsilon z)^2)-b^2(1+(\varepsilon z)^2)^2}{(1+\varkappa(\varepsilon z)^2)^2}.$$

The asymptotic solutions (as $\varepsilon\to 0$) to equation (4.5) have the following WKB structure:

$$\varphi=A(z)\exp\biggl\{\pm i\int\sqrt{p(z)}\,dz\biggr\}.$$

Each solution (defined by the sign in the exponent) can be continued in a certain way through the Stokes lines emanating from the turning points and dividing the complex plane z into sectors. For an eigenfunction to exist, the Stokes lines should have a certain structure that would guarantee a smooth transition from the decay for $z\to-\infty$ to the decay for $z\to+\infty$. Before studying the Stokes lines proper, consider the possible location of the turning points and poles of the function $p(z)$.

4.3. Turning points and branch points. The points in a neighborhood of which the WKB expansion is inapplicable are the zeros and poles of the function $p(z)$. The former are the turning points in a neighborhood of which the solution has the form of the Airy function, which determines the possibility of continuation of solutions across the Stokes lines. The latter, i.e., the poles of the function $p(z)$, are the attraction points of the Stokes lines, as will be shown below. Consider the location of these points. For convenience, using the terminology of WKB theory, we introduce the "slow variable" $\zeta = \varepsilon z$. Then the function p can be expressed as

$$p(\zeta,\omega) = \frac{c(1+\zeta^2)(1+\varkappa\zeta^2) - b^2(1+\zeta^2)^2}{(1+\varkappa\zeta^2)^2},$$

and equation (4.5), as

$$\varepsilon^2 \frac{d^2\varphi}{d\zeta^2} + p(\zeta,\omega)\varphi = 0. \tag{4.6}$$

4.3.1. *Turning points.* The zeros ζ^0 of the function $p(\zeta)$ are determined from the equation

$$(c\varkappa - b^2)\zeta^4 + \big(c(\varkappa+1) - 2b^2\big)\zeta^2 + (c - b^2) = 0, \tag{4.7}$$

i.e.,

$$\zeta^0_{1,2,3,4} = \pm\sqrt{\frac{\pm\sqrt{(c(\varkappa+1)-2b^2)^2 - 4(c\varkappa - b^2)(c-b^2)} - (c(\varkappa+1)-2b^2)}{2(c\varkappa - b^2)}}.$$

In a neighborhood of each turning point, equation (4.6) has the form of the Airy equation, and its solutions define a rule for continuing the solution across the Stokes lines.

In [24], Le Dizès et al. showed that in the presence of two turning points and in the absence of poles of the function $p(z)$, there exists a countable set of eigenfrequencies each of which corresponds to a structure of the Stokes lines for which the turning points are connected in a certain way by a common Stokes line (Fig. 6). The limit case of such a configuration is a multiple turning point. The eigenfrequencies lie in a neighborhood of a curve (in the complex plane ω) that ends at the frequency ω_{s} corresponding to this limit case (Fig. 6). Under some additional conditions, this frequency ω_{s} corresponds to the fastest growing mode; i.e., it is the highest point on the curve (Fig. 6b). However, in the general case it may not be a maximum point of $\operatorname{Im}\omega$ (Fig. 6a); moreover, it may even happen that $\operatorname{Im}\omega_{\mathrm{s}} < 0$, but a part of the curve lies in the upper half-plane and the system is unstable. In the present paper, we only study the condition $\operatorname{Im}\omega_{\mathrm{s}} > 0$ and construct the corresponding eigenfunction; we will show that this condition coincides with a necessary condition for global instability. As a result, we obtain a necessary and sufficient condition for global instability; however, it is unknown whether the eigenfunction demonstrated is the fastest growing one.

Thus, below we will consider a situation when two turning points merge. We find out which frequencies lead to multiple turning points.

1. *An internal root vanishes*:

$$\big(c(\varkappa+1) - 2b^2\big)^2 - 4(c\varkappa - b^2)(c-b^2) = c^2(\varkappa-1)^2 = 0.$$

This implies that $c(\omega) = 0$; hence, either $\omega = 0$ or $\omega = -16in/(\pi\,\mathsf{Re})$. Thus, such a configuration of turning points cannot give rise to a growing eigenfunction.

2. *An external root vanishes*: $c\varkappa = b^2$ *or* $c = b^2$. The first case is degenerate: the leading coefficient of equation (4.7) vanishes; i.e., two turning points go to infinity. Here we do not consider

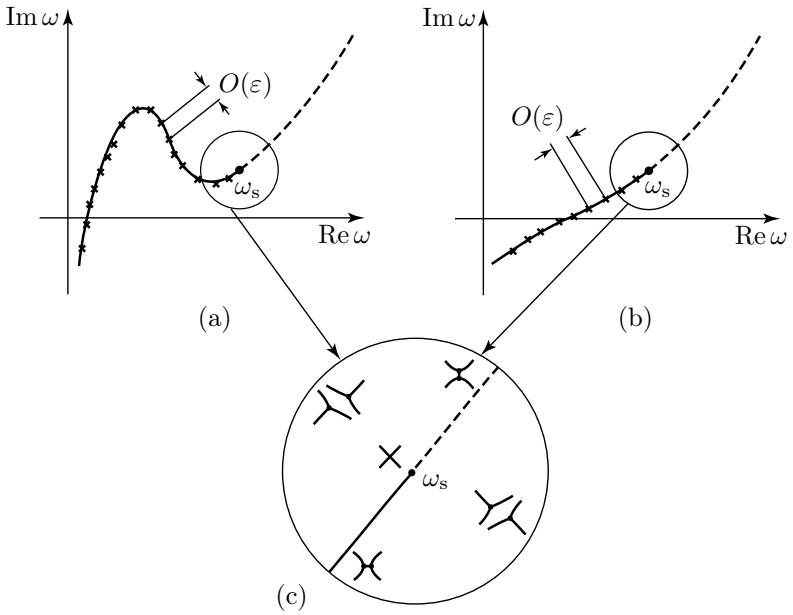

Fig. 6. Asymptotic (as $\varepsilon \to 0$) curve in the complex plane ω which corresponds to a situation when two turning points are connected by a common Stokes line and give rise to an eigenfunction (solid line) or are connected but do not give rise to an eigenfunction (dashed line). The position of eigenfrequencies for finite ε is shown by crosses. The frequency ω_{s} corresponds to a multiple turning point. The fastest growing eigenfunction corresponds to (a) a nonmultiple or (b) a multiple turning point. Part (c) shows separately the qualitative structure of the Stokes lines in a neighborhood of ω_{s}. The figure is reproduced from [24].

this case, because it is not of general character. The second case corresponds to the merging of two turning points at $\zeta = 0$, the other two points being located at $\zeta = \pm i$:

$$\zeta_{1,2}^0 = 0, \qquad \zeta_{3,4}^0 = \pm i.$$

Let us find frequencies $\omega = \omega_{\mathrm{s}}$ to which this configuration corresponds. Writing the equation $c(\omega) = b^2(\omega)$, we arrive at the following quadratic equation for the frequency:

$$\left(\beta_0 - \beta_{\mathrm{div}} + \frac{4(3n+1)^2}{\pi^2(2n+1)^2}\right)\omega^2 + i\omega\left(\frac{16n}{\pi\,\mathsf{Re}}(\beta_0 - \beta_{\mathrm{div}}) - \frac{32(1-9n^2)}{\pi^3(2n+1)\,\mathsf{Re}}\right) - \frac{64(1-3n)^2}{\pi^4\,\mathsf{Re}^2} = 0. \quad (4.8)$$

Since the leading coefficient is positive, the middle one is purely imaginary, and the constant term is negative, it follows that $\operatorname{Im}\omega_{\mathrm{s}}$ is positive if the imaginary part of the middle coefficient is negative:

$$\frac{16n}{\pi\,\mathsf{Re}}(\beta_0 - \beta_{\mathrm{div}}) - \frac{32(1-9n^2)}{\pi^3(2n+1)\,\mathsf{Re}} < 0.$$

Explicitly expressing β, we find that two turning points merge at $\zeta = 0$ for $\operatorname{Im}\omega_{\mathrm{s}} > 0$ if

$$\beta_0 < \beta_{\mathrm{abs}},$$

i.e., if the instability in the weakest place of the tube is absolute.

Note that the solutions ω_{s} to equation (4.8) have nonzero real part; i.e., the growing mode is of time-oscillating character.

4.3.2. *Poles of the function $p(\zeta)$.* The poles of $p(\zeta)$ are obviously given by the formula

$$\zeta_{\pm}^{\mathrm{p}} = \pm\frac{i}{\sqrt{\varkappa}}.$$

Consider equation (4.6) in a neighborhood of any of these points. Let $\zeta = \zeta^{\mathrm{p}} + \xi$, $|\xi| \ll |\zeta^{\mathrm{p}}|$, be an internal variable in a neighborhood of ζ^{p}. Substituting it into the equation and retaining only the leading term of the expansion of $p(\zeta)$, we obtain

$$p(\xi) = \frac{b^2(\varkappa-1)^2}{\varkappa^3}\frac{1}{\xi^2}.$$

Then equation (4.6) takes the form

$$\frac{d^2\varphi}{d\xi^2} + \frac{b^2(\varkappa-1)^2}{\varepsilon^2\varkappa^3}\frac{1}{\xi^2}\varphi(\xi) = 0. \tag{4.9}$$

The exact solution of this equation is

$$\varphi(\xi) = \xi^{\alpha}, \qquad \alpha = \frac{1 \pm i\sqrt{4\lambda-1}}{2}, \qquad \lambda = \frac{b^2(\varkappa-1)^2}{\varepsilon^2\varkappa^3}. \tag{4.10}$$

Since the local wave number for problem (4.9) has the form

$$k_{1,2}(\xi) = \pm\frac{\sqrt{\lambda}}{\xi}, \tag{4.11}$$

the WKB approximation to the solution is given by

$$\varphi_{\mathrm{WKB}}(\xi) = \exp\biggl\{i\int k_j(\xi)\,d\xi\biggr\} = \xi^{\pm i\sqrt{\lambda}}.$$

One can see that

$$\frac{\varphi_{\mathrm{WKB}}(\xi)}{\varphi(\xi)} = \xi^{\frac{1}{2}+o(1)}, \qquad \varepsilon \to 0.$$

Thus, the relative error of φ and φ_{WKB} tends to zero as the distance from ζ^{p} grows.

Consider the arrangement of the lines

$$\operatorname{Im}\int \bigl(k_1(\xi) - k_2(\xi)\bigr)\,d\xi = \mathrm{const},$$

which are the Stokes lines in a neighborhood of the point ζ^{p}. In view of (4.11), these lines are described by the equation

$$\operatorname{Re}\bigl(\sqrt{\lambda}\ln\xi\bigr) = \operatorname{Re}\sqrt{\lambda}\ln|\xi| - \operatorname{Im}\sqrt{\lambda}\arg\xi = \mathrm{const}.$$

Hence one can see that these lines are spirals rotating around the point ζ^{p}. Thus, the Stokes line entering a neighborhood of one of the points ζ^{p} cannot then leave it but indefinitely spirals and approaches ζ^{p}. In contrast to the turning points, where one can analyze a single-valued exact solution (Airy function) in a neighborhood of a turning point in order to eliminate the nonuniqueness of the WKB solution, the nonuniqueness arising here is also characteristic of the exact solution $\varphi(\xi)$ (4.10) and, hence, cannot be eliminated in principle: the eigenfunctions of problem (4.5) are multivalued. Below, using cuts emanating from the points ζ^{p}, we choose a single-valued branch of the eigenfunction that is defined on the whole "physical" real z-axis.

4.4. Structure of Stokes lines. The location of the Stokes lines defined by the equation

$$\operatorname{Im}\int_{\zeta^0}^{\zeta} \bigl(k_1(\zeta) - k_2(\zeta)\bigr)\,d\zeta = 0,$$

where ζ^0 is a turning point, was calculated numerically. Since the variation of the parameters does not give rise to any singularities in equation (4.5), the topology of the Stokes lines does not change

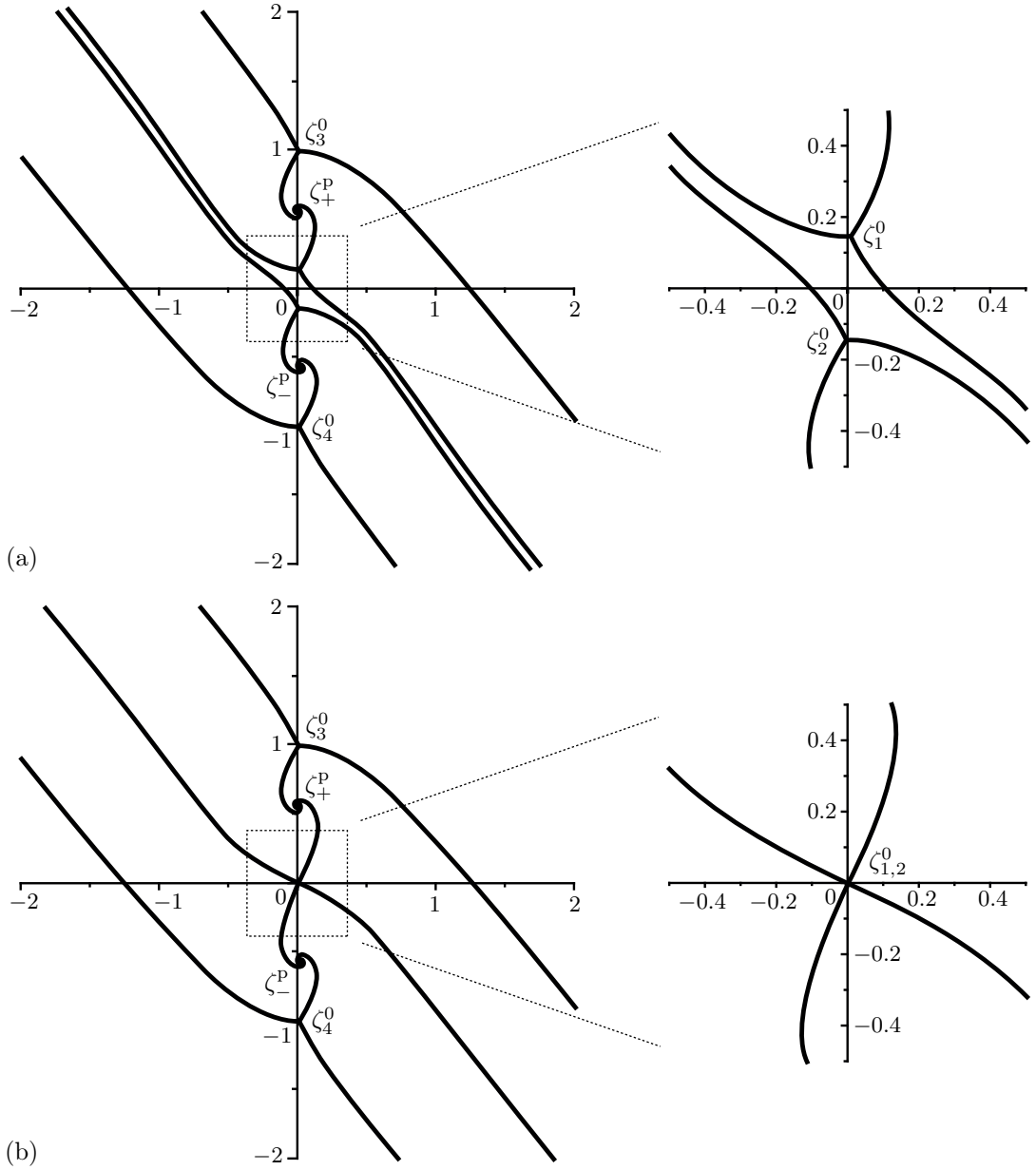

Fig. 7. Stokes lines in the complex plane z for ω (a) close to ω_{s} and (b) equal to ω_{s}.

and it suffices to consider only one set of parameters. The calculations were performed for

$$n = 0.2, \qquad \beta_0 = 0.347, \qquad \beta_1 = 1.115. \tag{4.12}$$

For this value of n we have $\beta_{\mathrm{fl}} = 0.897$ and $\beta_{\mathrm{abs}} = 0.463$, so absolute instability occurs for β_0 and stability occurs for β_1. Equation (4.8) has solutions inversely proportional to the Reynolds number Re, and the function $p(\zeta)$ is inversely proportional to its square. Therefore, an arbitrary number can be taken as the value of Re in calculations; this does not affect the structure of the Stokes lines. For convenience, we took $\mathsf{Re} = 1$. Then equation (4.8) has the following roots: $\omega_{\mathrm{s}} \approx \pm 0.3378 + 0.155i$. To calculate the Stokes lines, we took a value with positive real part.

To understand the structure of the Stokes lines, we first consider the results of calculations for the frequency $\omega = 0.337 + 0.165i$, which is close but not equal to ω_{s} (Fig. 7a). One can see that there are four turning points ζ^0, two of which ($\zeta_{1,2}^0$) are located near $\zeta = 0$, while the other

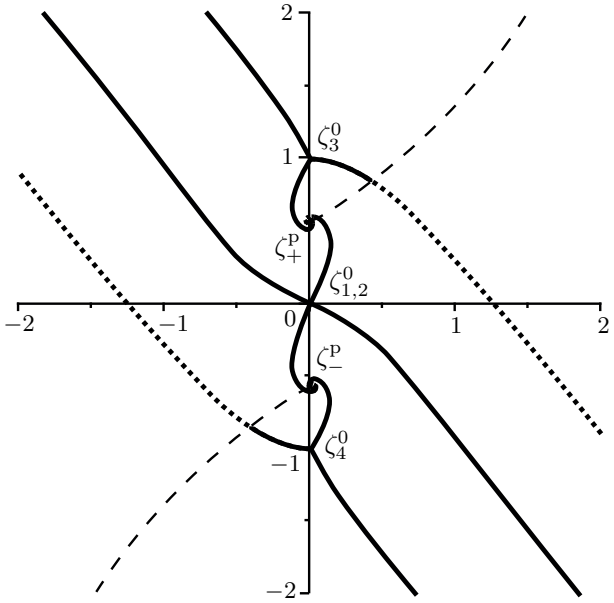

Fig. 8. Stokes lines in the complex plane z for $\omega = \omega_{\mathrm{s}}$, and cuts emanating from the points $\zeta = \zeta^{\mathrm{p}}$. The cuts are shown by dashed lines; the Stokes lines that continue on another sheet of the Riemann surface are shown by dotted lines.

two ($\zeta_{3,4}^0$) are near $\zeta = \pm i$. The function $p(\zeta)$ has two poles $\zeta_{\pm}^{\mathrm{p}}$. One can see that there are three Stokes lines emanating from each turning point, two of which go to infinity and tend asymptotically to straight lines, while one is wound spirally around one of the points $\zeta_{\pm}^{\mathrm{p}}$. As ω tends to ω_{s}, the turning points $\zeta_{1,2}^0$, which are close to 0, approach each other and merge together for $\omega = \omega_{\mathrm{s}}$, giving the structure of the Stokes lines shown in Fig. 7b.

Since the branching of the solution in a neighborhood of the points ζ^{p} yields an infinite-valued function, one should make cuts as shown in Fig. 8 to construct a smooth eigenfunction along the z-axis. As a result, the Stokes lines emanating from the turning points $\zeta_{3,4}^0 = \pm i$ do not reach the real axis: one line recedes from this axis, another is wound around one of the points ζ^{p} and after each turn goes to the next sheet of the Riemann surface, and the third line crosses the cut prior to intersecting the real axis and goes to another sheet. As a result, the picture in the neighborhood of the real axis looks as if there were only two multiple turning points $\zeta_{1,2}^0 = 0$. Such a configuration corresponds to the existence of an eigenfunction, and the role of the neighborhood of a multiple turning point consists in guaranteeing a smooth "switching" from the decay for $z \to -\infty$ to the decay for $z \to +\infty$.

As a result, we have proved that for $\omega = \omega_{\mathrm{s}}$ equation (4.5) has a global eigenfunction, i.e., a nonzero solution that decays for $z \to \pm\infty$.

4.5. Decay condition for $Q''(z)$. Since $p(z) \to (c\varkappa - b^2)/\varkappa^2$ as $z \to \pm\infty$, the decay of the function $\varphi(z)$ has the form

$$\varphi(z) \sim \exp\left\{\pm\frac{\sqrt{b^2 - c\varkappa}}{\varkappa} z\right\}.$$

However, we should also check that the original unknown function $Q''(z)$ decays. Applying formula (4.4), we have

$$Q''(z) \sim \exp\left\{\frac{-b \pm \sqrt{b^2 - c\varkappa}}{\varkappa} z\right\}.$$

Table 1. Eigenfrequencies for the parameters (4.12) and various values of ε

ε^2	ω
1	$0.3838 + 0.0930\,i$
0.1	$0.3596 + 0.1313\,i$
0.01	$0.3454 + 0.1471\,i$
0.001	$0.3403 + 0.1528\,i$
Asymptotics	$0.3378 + 0.1550\,i$

In the case corresponding to a multiple turning point, we have $c(\omega) = b^2(\omega)$, so the decay condition for the function Q'' reduces to

$$|\operatorname{Re} b| < |\operatorname{Im} b|\sqrt{\varkappa - 1}. \tag{4.13}$$

Substituting here the eigenfunction frequency $\omega = \omega_{\mathrm{s}}$, i.e., the solution of equation (4.8), we obtain the inequality

$$\frac{\beta_1 - \beta_0}{\beta_0 - \beta_{\mathrm{div}}(n)} > \frac{(n+1)^2}{4(3n+1)^2n^2}\,\frac{\left(\beta_0\pi^2 - \frac{2(3n+1)}{2n+1}\right)^2}{\frac{(3n-1)^2(6n^2+3n+1)^2}{4n^4(2n+1)^2} - \left(\beta_0\pi^2 + \frac{6n^3-n^2-1}{2(2n+1)n^2}\right)^2}.$$

This relation is too cumbersome to be studied analytically. Therefore, for the minimum value of β_1, $\beta_1 = \beta_{\mathrm{fl}}(n)$, and for the whole range $\beta_{\mathrm{div}}(n) < \beta_0 < \beta_{\mathrm{abs}}(n)$ of β_0, we verified numerically that this inequality is always satisfied in the interval $0 < n < 1/3$; hence, it holds for all $\beta_1 > \beta_{\mathrm{fl}}(n)$. Thus, this inequality does not impose additional constraints on the values of the parameters, and $Q''(z)$ always decays when $\varphi(z)$ decays.

Thus, for small ε, for a tube conveying a fluid to be globally unstable, i.e., for equation (4.3) to have an increasing eigenfunction, the following condition is sufficient: the local instability in the weakened region is absolute. The same condition is necessary for global instability [9]; therefore, this condition is necessary and sufficient for the problem under consideration.

Note that there exists a family of other eigenfunctions in which two turning points do not merge but are connected by a common Stokes line. In the present study, we do not analyze this family, because the existence of at least one growing eigenfunction is sufficient for instability.

4.6. Direct numerical solution of the equation for perturbations. To verify the asymptotic results obtained and assess how the value of ε affects the value of the eigenfrequency, we solved the eigenvalue problem numerically for the parameters (4.12) on the interval $\zeta \in [L, 0]$. In the calculations, we took $L = -5$, because in this case $\beta(L)$ is close to the asymptotic value of β_1 and the solutions (4.6) for $\zeta < L$ are close to the exponential functions $\exp\{\pm i\sqrt{p_\infty}\,\zeta/\varepsilon\}$, where p_∞ is the limit value of $p(\zeta)$ as $\zeta \to -\infty$. For $\zeta = L$, we defined the values

$$\varphi = 1, \qquad \frac{d\varphi}{dz} = \frac{i\sqrt{p_\infty}}{\varepsilon}$$

(the branch of the root was chosen so that $\operatorname{Im}\sqrt{p_\infty} > 0$, which guaranteed the decay of the solution as $\zeta \to -\infty$) and integrated equation (4.6) numerically up to $\zeta = 0$. For various values of ε in a neighborhood of ω_{s}, we sought a frequency ω such that

$$\frac{d\varphi(0)}{d\zeta} = 0.$$

Under this condition, the solution can be symmetrically extended to the domain $\zeta > 0$ with a continuous second derivative at $\zeta = 0$, thus providing an even eigenfunction. Table 1 presents

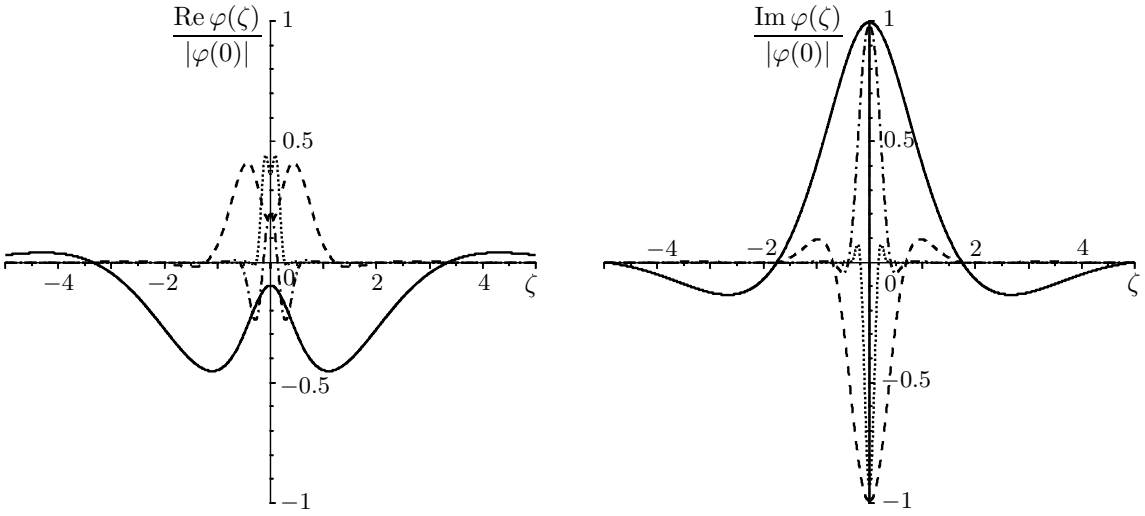

Fig. 9. Eigenfunctions $\varphi(\zeta)$ of equation (4.6) for the parameters (4.12) and $\varepsilon^2 = 1$ (solid curve), $\varepsilon^2 = 0.1$ (dashed curve), $\varepsilon^2 = 0.01$ (dot–dash curve), and $\varepsilon^2 = 0.001$ (dotted curve).

the results of calculations, and Fig. 9 demonstrates the graphs of the corresponding eigenfunctions normalized by their absolute values at zero. As expected according to the WKB approximation, the eigenfunctions are concentrated about $\zeta = 0$. One can see that as ε decreases, the calculated values of frequencies tend to the asymptotic value. Moreover, instability occurs even for $\varepsilon = 1$, and the value of frequency for $\varepsilon = 1$ is fairly close to the asymptotic value.

5. CONCLUSIONS

We have studied the stability loss unrelated to the separation of flow from the tube walls and to the loss of axial symmetry of the tube. For an infinitely long uniform tube, we have found the regions of ordinary and absolute instability. These regions exist for the power-law indices $n < 0.611$ and $n < 1/3$, respectively; thus, only pseudoplastic flow may lead to instability, while, for example, the linear viscous flow ($n = 1$) is stable with respect to the perturbations under consideration.

For an infinitely long nonuniform tube of constant radius whose stiffness varies slowly in space in such a way that there is a "weakened" locally unstable region of finite length, we have obtained a sufficient condition for global instability, which coincides with the known necessary condition: the tube is globally unstable if and only if the local instability in the most weakened region is absolute; otherwise the local instability is suppressed by the surrounding locally stable regions.

The growing eigenfunction constructed in the paper corresponds to a multiple turning point; it is localized in the "weakest" region. The question of whether this eigenfunction is the fastest growing one remains open: there exists a family of eigenfunctions that has not been considered here in which two turning points are connected by a common Stokes line. It is also of interest how far one can "move" two turning points away from each other while keeping the eigenfunctions growing and how this is related to the distribution of local stability properties of the tube.

ACKNOWLEDGMENTS

The research of V. V. Vedeneev is supported by the Russian Science Foundation under grant 14-50-00005 and performed in the Steklov Mathematical Institute of Russian Academy of Sciences. He wrote Sections 1 and 4. Sections 2 and 3 are written by A. B. Poroshina.

REFERENCES

1. M. V. Abakumov, I. V. Ashmetkov, N. B. Esikova, V. B. Koshelev, S. I. Mukhin, N. V. Sosnin, V. F. Tishkin, A. P. Favorsky, and A. B. Khrulenko, "Strategy of mathematical cardiovascular system modeling," Mat. Model. **12** (2), 106–117 (2000).
2. M. Anand and K. R. Rajagopal, "A shear-thinning viscoelastic fluid model for describing the flow of blood," Int. J. Cardiovasc. Med. Sci. **4** (2), 59–68 (2004).
3. A. M. Barlukova, A. A. Cherevko, and A. P. Chupakhin, "Traveling waves in a one-dimensional model of hemodynamics," Prikl. Mekh. Tekh. Fiz. **55** (6), 16–26 (2014) [J. Appl. Mech. Tech. Phys. **55**, 917–926 (2014)].
4. A. Bers, "Space-time evolution of plasma instabilities—absolute and convective," in *Handbook of Plasma Physics*, Ed. by A. A. Galeev and R. N. Sudan (North-Holland, Amsterdam, 1983), Vol. 1, pp. 451–517.
5. C. D. Bertram, C. J. Raymond, and T. J. Pedley, "Mapping of instabilities for flow through collapsed tubes of differing length," J. Fluids Struct. **4** (2), 125–153 (1990).
6. C. D. Bertram and J. Tscherry, "The onset of flow-rate limitation and flow-induced oscillations in collapsible tubes," J. Fluids Struct. **22** (8), 1029–1045 (2006).
7. R. J. Briggs, *Electron-Stream Interaction with Plasmas* (MIT Press, Cambridge, MA, 1964).
8. *Cardiovascular Mathematics: Modeling and Simulation of the Circulatory System*, Ed. by L. Formaggia, A. Quarteroni, and A. Veneziani (Springer, Milano, 2010), Model. Simul. Appl. **1**.
9. J.-M. Chomaz, P. Huerre, and L. G. Redekopp, "A frequency selection criterion in spatially developing flows," Stud. Appl. Math. **84** (2), 119–144 (1991).
10. P.-P. L. O. Coene, A. K. Groen, P. H. P. Davids, M. Hardeman, G. N. J. Tytgat, and K. Huibregtse, "Bile viscosity in patients with biliary drainage. Effect of co-trimoxazole and N-acetylcysteine and role in stent clogging," Scand. J. Gastroenterol. **29** (8), 757–763 (1994).
11. L. Formaggia, D. Lamponi, and A. Quarteroni, "One-dimensional models for blood flow in arteries," J. Eng. Math. **47**, 251–276 (2003).
12. G. P. Galdi, R. Rannacher, A. M. Robertson, and S. Turek, *Hemodynamical Flows: Modeling, Analysis and Simulation* (Birkhäuser, Basel, 2008).
13. F. J. H. Gijsen, F. N. van de Vosse, and J. D. Janssen, "The influence of the non-Newtonian properties of blood on the flow in large arteries: Steady flow in a carotid bifurcation model," J. Biomech. **32** (6), 601–608 (1999).
14. A. G. Gorshkov, V. I. Morozov, A. T. Ponomarev, and F. N. Shklyarchuk, *Aerohydroelasticity of Designs* (Fizmatlit, Moscow, 2000) [in Russian].
15. J. B. Grotberg and O. E. Jensen, "Biofluid mechanics in flexible tubes," Annu. Rev. Fluid Mech. **36**, 121–147 (2004).
16. M. Heil and J. Boyle, "Self-excited oscillations in three-dimensional collapsible tubes: Simulating their onset and large-amplitude oscillations," J. Fluid Mech. **652**, 405–426 (2010).
17. M. Heil and A. L. Hazel, "Fluid-structure interaction in internal physiological flows," Annu. Rev. Fluid Mech. **43**, 141–162 (2011).
18. O. E. Jensen, "Instabilities of flow in a collapsed tube," J. Fluid Mech. **220**, 623–659 (1990).
19. O. E. Jensen and T. J. Pedley, "The existence of steady flow in a collapsed tube," J. Fluid Mech. **206**, 339–374 (1989).
20. A. I. Katz, Y. Chen, and A. H. Moreno, "Flow through a collapsible tube: Experimental analysis and mathematical model," Biophys. J. **9** (10), 1261–1279 (1969).
21. D. N. Ku, "Blood flow in arteries," Annu. Rev. Fluid Mech. **29**, 399–434 (1997).
22. A. G. Kuchumov, V. Gilev, V. Popov, V. Samartsev, and V. Gavrilov, "Non-Newtonian flow of pathological bile in the biliary system: Experimental investigation and CFD simulations," Korea–Aust. Rheol. J. **26** (1), 81–90 (2014).
23. R. B. Kudenatti, N. M. Bujurke, and T. J. Pedley, "Stability of two-dimensional collapsible-channel flow at high Reynolds number," J. Fluid Mech. **705**, 371–386 (2012).
24. S. Le Dizès, P. Huerre, J. M. Chomaz, and P. A. Monkewitz, "Linear global modes in spatially developing media," Philos. Trans. R. Soc. London A **354** (1705), 169–212 (1996).
25. H. F. Liu, X. Y. Luo, and Z. X. Cai, "Stability and energy budget of pressure-driven collapsible channel flows," J. Fluid Mech. **705**, 348–370 (2012).
26. X. Y. Luo and T. J. Pedley, "Multiple solutions and flow limitation in collapsible channel flows," J. Fluid Mech. **420**, 301–324 (2000).
27. A. Marzo, X. Y. Luo, and C. D. Bertram, "Three-dimensional collapse and steady flow in thick-walled flexible tubes," J. Fluids Struct. **20** (6), 817–835 (2005).
28. A. B. Metzner and J. C. Reed, "Flow of non-Newtonian fluids—Correlation of the laminar, transition, and turbulent-flow regions," AIChE J. **1** (4), 434–440 (1955).

29. J. E. Moore Jr., S. E. Maier, D. N. Ku, and P. Boesiger, "Hemodynamics in the abdominal aorta: A comparison of in vitro and in vivo measurements," J. Appl. Physiol. **76** (4), 1520–1527 (1985).
30. M. P. Païdoussis, *Fluid-Structure Interactions: Slender Structures and Axial Flow* (Academic, San Diego, CA, 1998), Vol. 1.
31. T. J. Pedley, "Arterial and venous fluid dynamics," in *Cardiovascular Fluid Mechanics*, Ed. by G. Pedrizzetti and K. Perktold (Springer, Wien, 2003), pp. 1–72.
32. T. J. Pedley, B. S. Brook, and R. S. Seymour, "Blood pressure and flow rate in the giraffe jugular vein," Philos. Trans. R. Soc. London B: Biol. Sci. **351** (1342), 855–866 (1996).
33. P. Reymond, F. Merenda, F. Perren, D. Rüfenacht, and N. Stergiopulos, "Validation of a one-dimensional model of the systemic arterial tree," Am. J. Physiol. Heart Circ. Physiol. **297** (1), 208–222 (2009).
34. A. H. Shapiro, "Physiological and medical aspects of flow in collapsible tubes," in *Proc. 6th Canadian Congress of Applied Mechanics* (Univ. Br. Columbia, Vancouver, 1977), pp. 883–906.
35. S. S. Simakov, A. S. Kholodov, and A. V. Evdokimov, "Methods of calculation of global blood flow in a human body involving heterogeneous computation models," in *Medicine in the Mirror of Informatics* (Nauka, Moscow, 2008), pp. 124–170 [in Russian].
36. N. P. Smith, A. J. Pullan, and P. J. Hunter, "An anatomically based model of transient coronary blood flow in the heart," SIAM J. Appl. Math. **62** (3), 990–1018 (2002).
37. Yu. Vassilevski, S. Simakov, V. Salamatova, Yu. Ivanov, and T. Dobroserdova, "Numerical issues of modelling blood flow in networks of vessels with pathologies," Russ. J. Numer. Anal. Math. Model. **26** (6), 605–622 (2011).
38. R. J. Whittaker, M. Heil, O. E. Jensen, and S. L. Waters, "Predicting the onset of high-frequency self-excited oscillations in elastic-walled tubes," Proc. R. Soc. London A **466**, 3635–3657 (2010).
39. V. S. Yushutin, "Stability of flow of a nonlinear viscous power-law hardening medium in a deformable channel," Vestn. Mosk. Univ., Ser. 1: Mat., Mekh., No. 4, 67–70 (2012) [Moscow Univ. Mech. Bull. **67** (4), 99–102 (2012)].

Translated by I. Nikitin